IEEE Access
Multidisciplinary | Rapid Review | Open Access Journal

Received June 5, 2017, accepted August 8, 2017, date of publication August 31, 2017, date of current version September 27, 2017.

Digital Object Identifier 10.1109/ACCESS.2017.2741338

Adaptive De-Coupling and Multi-BS Association in Heterogeneous Networks

AYSHA EBRAHIM[1], (Member, IEEE), AND EMAD ALSUSA[2], (Senior Member, IEEE)
[1]University of Bahrain Sakhir Campus, Sakhir 32038, Bahrain
[2]Manchester University, Manchester M60 1QD, U.K.

Corresponding author: Aysha Ebrahim (amebrahim@uob.edu.bh)

ABSTRACT This paper proposes a novel method for maximizing the spatial frequency reuse in cellular networks by exploiting the possibility to simultaneously associate each user to multiple base-stations (BSs). To this end, the proposed technique presents a criterion for determining when a user should be associated with one or more BSs and whether the uplink and downlink should be decoupled, based on minimizing the average interference power across the network. To minimize the effect of interference that may occur due to increasing the spatial frequency reuse, the proposed association methods are integrated with an overlap checking scheme to insure that the resources are orthogonalized between the interfering BSs and user equipments. The results show that significant performance improvements can be attained by the proposed scheme in comparison with other benchmark techniques.

INDEX TERMS Femtocell, heterogeneous network, interference avoidance, LTE, OFDMA, resource management, user association.

I. INTRODUCTION

The rapid evolution in mobile communication systems has increased the burden on network operators to deal with the sharp increase in data rate requirements. One of the popular solutions to improve the capacity of cellular systems is to deploy small low-cost cells, such as femtocells and picocells, within the cellular hierarchy to improve the signal quality by reducing the distance between the BSs and the users [1]. Despite the promising gain that can be attained by small cells, the ad-hoc nature of the deployment of such cells introduces several threats for the network operators. Cross-tier and co-tier interference are major challenges that result from the unplanned deployment of small cells [2]. Co-tier interference results from the densification of small cells which generates a large number of overlapped cell boundaries. On the other hand, excessive cross-tier interference caused by the macrocell can seriously degrade the performance of the low power small cells. To minimize the effect of such interference, inter-cell interference coordination (ICIC) schemes need to be employed to orthogonalize the allocation of the potential interfering parties. However, orthogonalization comes with the drawback of restricting the frequency reuse of the system. Therefore ICIC methods need to be supported by other strategies to improve the resource utilization and enhance the overall throughput. One possible solution for improving the throughput of wireless networks is to integrate ICIC with advanced cellular association techniques. The traditional approach for user association is to simply connect users with the BSs that are offering the strongest received signal power [3]. Unfortunately, considering the received signal power only to conduct the association might be ineffective due to the random nature of femtocells deployment which yields unbalanced load distribution where some cells become highly loaded while others are left underutilized.

As such, a number of cellular association schemes have been suggested for cellular networks in the literature. The authors in [4], proposed a method based on semi-markov decision process (SMDP), where a distributed load-balancing and admission control algorithm is developed to improve the overall network throughput while imposing blocking probability constraints on users to control the performance degradation. The authors in [5], investigated a cellular association and handover problem in femtocell networks to maximize the network throughput and fairness. In [6], the authors presented a sleep mode and handover management technique to reduce the interference and increase capacity of femtocell networks by running a sequence of tests to determine the cells to be switched off, and the cells to which the users of cells in sleep mode will handover to. In [7] and [8], the authors considered a cellular association scheme for heterogeneous deployment

in which the cellular association is performed based on range expansion taking into consideration the transmit power variability between the macrocell and small cells.

Furthermore, the concept of coupled user association was dominant for decades in cellular systems where mobile users are bound to connect to the same BS in the UL and DL. Recent research trends began to rethink this concept and investigate the benefits of UL/DL decoupling for improving the throughput gain [9]. The authors in [10] presented a decoupled UL and DL method that takes into consideration parameters such as the UL pathloss and the cell loads. In [11], the authors discussed UL user association for optimizing users packet success rate using game theory while, in [12], a mathematical model is introduced to investigate the impact of decoupling the UL from the DL association where it was shown that minimum pathloss based UL association is an ideal strategy to improve the UL rate.

In addition to the UL/DL decoupling, incorporating transmission diversity can be greatly beneficial for improving cellular systems performance. With transmission diversity, users are allowed to be jointly processed by several BSs rather than being restricted to connect with only one BS. The author in [13] presented a multi-point transmission technique for improving the UL capacity. Users transmit in the UL to a group of macrocells that are virtually connected to process the UL transmissions by cooperating with each other. The authors in [14] presented an interference alignment (IA) based approach, in which the transmission is coordinated between BSs and users to avoid the limiting effect of interference that results from simultaneous transmissions.

In this paper, we propose a novel adaptive decoupling and multi-BS association technique that allows users to be connected to multiple BSs to maximize the spatial frequency reuse by allowing users access to more resources. The algorithm determines whether the association between BSs and users in the UL session should be coupled/decoupled from the DL in addition to introducing a mechanism to decide whether users should be associated to a single BS or multiple BSs simultaneously in a similar manner to multi-stream multi-BS interference alignment scenarios [14]. Unlike IA systems however, where interference is managed in the Physical layer, in this case interference is managed in the MAC layer through threshold dependent resource orthogonalization as will be demonstrated later. Furthermore, the investigated association schemes are augmented with a tailor-made overlap checking scheme used as a means to control the interference that may arise as a result of increasing the frequency reuse in the system. The proposed approach is both network- and user-centric, in which we aim to maximize the total network capacity as well as the capacity per user. To the best of our knowledge, the idea of joint decoupling and multi-BS association has not been addressed before in the literature.

The paper is structured as follows. Section II discusses the system model. Section III discusses the interference aware user association method. In section IV, the adaptive decoupling and multi-BS association framework is presented to optimize the user association in the network. Section V analyzes the impact of the coverage on the users association. Section VI provides results and discussion. Finally, a summary for this chapter is provided in section VII.

II. SYSTEM MODEL AND ASSUMPTIONS

An orthogonal frequency-division multiple access (OFDMA) system is considered with a network featuring a macrocell and a set of small BSs and users with a total of B BSs and K users. Assume $\mathcal{B}$ and $\mathcal{K}$ are the sets of BSs and users in which i and j denote two arbitrary BSs from the set $\mathcal{B}$, j refers to a neighboring BS of i and k is a random user from the set $\mathcal{K}$. The system bandwidth is divided into N orthogonal physical resource blocks (PRBs) and each BS performs frequency allocation to its connected users independently using CQI reports sent from the users. It is presumed that time-division duplex (TDD) is employed which separates the UL and DL transmission in time and therefore the transmissions in one session do not interfere with the other. Each user from the set $\mathcal{K}$ is allowed to be associated with a maximum of two BSs in each session as it is less likely that a user is located in the coverage area of more than two BSs as shown in fig. 1. The notation K_i represents the number of users associated with BS i. Same cell users occupy orthogonal resources and therefore the effect of intra-cell interference can be neglected. A full-buffer model is used to form the user traffic and the channel variation is represented using Rayleigh fading to model the impact of the propagation environment on the radio signal.

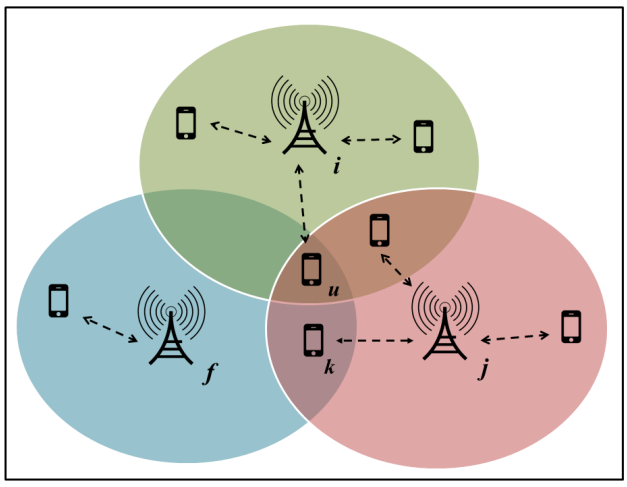

FIGURE 1. Illustration of SMBA association scheme.

A. DOWNLINK SIGNAL MODEL

Assuming the DL received power from BS i to user k at PRB n is denoted by $\Gamma_{i,k,n}$, the channel between i and k is referred to as $\hbar_{i,k,n}$, η_0 is the AWGN and $\Gamma_{j,k,n}$ is the interference power received from neighboring BS j to user k at PRB n. Then, the DL signal-interference-plus-noise ratio (SINR) achieved by user k connected to BS i at PRB n can be expressed as

$$\Upsilon_{i,k,n} = \frac{\Gamma_{i,k,n}.\hbar_{i,k,n}}{\eta_0 + \sum_{j=1}^{B} \Gamma_{j,k,n}.\hbar_{j,k,n}}, \qquad j \neq i. \tag{1}$$

It is presumed that all BSs in the system transmit at the maximum power level and the transmission power is distributed equally among the PRBs. The users connect to the BSs offering the strongest DL received power and $\alpha^{dl} \in \mathbb{R}^{B\times K}$ is a vector that indicates the DL association between BSs and users

$$\alpha_{i,k}^{dl} = \begin{cases} 1, & \text{if user } k \text{ is associated with BS } i \\ 0, & \text{Otherwise} \end{cases} \quad (2)$$

B. UPLINK SIGNAL MODEL

In the UL, the received signal power from UE k to BS i at PRB n is referred to as $\Gamma_{k,i,n}$ and the received interference power from UE k to nearby BS j is represented by $\Gamma_{k,j,n}$. Thus, the UL SINR is given by

$$\Upsilon_{i,k,n} = \frac{\Gamma_{k,i,n}\hbar_{i,k,n}}{\eta_0 + \sum_{j=1}^{B}\sum_{k=1}^{S_j}\Gamma_{k,j,n}.\hbar_{j,k,n}}, \qquad j \neq i. \quad (3)$$

All UEs in the system are assumed to be transmitting at the maximum power level. Furthermore, $\alpha^{ul} \in \mathbb{R}^{B\times K}$ denotes a vector representing the association between the BSs and users in the UL which is defined as in eq. (2).

III. NETWORK CAPACITY MAXIMIZATION

The network capacity maximization (NCM) user association method presented in our previous work in [15] is expanded to perform the UL association as will be described in the next section. In NCM, the association decisions are selected to improve the overall network throughput. This section provides a brief description of the NCM association scheme.

A. RESOURCE PARTITIONING

The algorithm starts by dividing the available resources among all the users. Users that are residing in the coverage range of each BS $i \in \mathcal{B}$ are first identified as follows

$$\Phi_i(j,k) = \begin{cases} 1 & \frac{\Gamma_{i,k,n}}{\Gamma_{j,k,n}} < \beta \\ 0 & \text{Otherwise} \end{cases}, \quad \forall i,j \in \mathcal{B} \wedge k \in \mathcal{K} \quad (4)$$

where, the matrix $\Phi_i(j,k) \in \mathbb{R}^{B\times K}$ indicates whether user k is located in the range of BS j and β is the signal-to-interference (SIR) threshold.

Users are initially associated with the BSs based on Max-RSS association policy. The resources are then distributed among the users, where each BS calculates the maximum amount of resources it can offer to each user within its coverage, by dividing the total number of resources N, by the number of users detected within its coverage area from (4)

$$\Omega_i = N / \left(\sum_{k=1}^{K} \{\Phi(k,i) = 1\} \right). \quad (5)$$

where $\Omega_i \in \Omega_B$ and $\Omega_B = [\Omega_1, \ldots, \Omega_i, \ldots, \Omega_j, \ldots, \Omega_B]$.

A given user k may not be allocated the maximum number of resources offered from its serving BS i. For instance, if user k is located in the vicinity of BS j, the condition: $[\Omega_i + \Omega_j.K_j] \leq N$ is checked to prevent UE k from interfering with BS j's UEs where Ω_j represent the available resources a neighbouring BS j offers each of its users and K_j is the number of UEs connected to j. In case the condition is satisfied, which means that no overlap is detected, then the number of PRBs assigned to UE k , Ψ_k is set to Ω_i, otherwise, Ψ_k is reduced to Ω_j to prevent user k from interfering with BS j's UEs

$$\Psi_k = \begin{cases} \Omega_i, & [\Omega_i + \Omega_j.K_j] \leq N \\ \Omega_j, & \text{otherwise} \end{cases} \quad (6)$$

where the vector $\Psi_K = [\Psi_1, \ldots, \Psi_k \cdots \Psi_K]$ stores the number of resources dedicated for each user.

B. CAPACITY MAXIMIZATION

After determining the set of resources per user, the achievable capacity is then measured for the users that can be granted more resources from the neighboring BSs than from the original serving BS

$$\mathbb{C}_{j,k} = \begin{cases} \Psi_k.W.\log_2\left(1 + \Upsilon_{j,k,n}\right), & \text{if } \Omega_j > \Omega_i \\ 0, & \text{otherwise} \end{cases}, \quad (7)$$

where W refers to the bandwidth per PRB.

In case the achievable capacity at BS j is higher than that achieved at BS i, the condition $[\Omega_i + \Omega_j.K_j] \leq N$ is preformed again to check that the additional resources obtained from the new association do not overlap with any interfering neighbors. Among the candidate pairs that pass the aforementioned condition, the impact of associating these pairs on the overall network rate is determined and the pair that maximizes the overall network throughput is selected first. The process then repeats to search for other association pairs.

IV. ADAPTIVE DE-COUPLING AND MULTI-BS ASSOCIATION FRAMEWORK

The objective of the proposed adaptive De-Coupling and Multi-BS association framework is to optimize the user association to maximize frequency reuse and improve the UL and DL rates without deteriorating the QoS. The method is executed by a central unit to determine the optimal association and the resources are assigned to users based on the resource partitioning method discussed in sec. III where BSs use this information to perform the resource allocation.

A. COUPLING/DECOUPLING ASSOCIATION (CDA)

This section discusses the coupling/decoupling association (CDA) method which determines whether users in the UL session remain associated with the same BS in the DL or decoupled and associated with another BS. The coupling/decoupling of a user is determined relative to the capacity gain achieved when a user is decoupled compared to the coupled case, which is performed based on the NCM association method. Users initially connect with BSs based on max RSS. The neighboring BSs of a particular user k

are then determined based on the UL noise rise, in case the UL interference power from UE k received by BS j $\Gamma_{k,j,n}$, exceeds the noise rise threshold $\eta_0 + \sigma$ [16], then UE k is considered in proximity to BS j

$$\Theta_{j,k} = \begin{cases} 1 & \text{if } \Gamma_{k,j,n} > \eta_0 + \sigma \\ 0 & \text{Otherwise} \end{cases}, \tag{8}$$

where $\Theta \in \mathbb{R}^{B\times K}$ is a matrix that demonstrates the proximity of users and BSs in the UL and σ refers to the noise rise (e.g., 10 dB). The resource as assigned to users based on the resource partitioning method discussed in the previous section. For each $\Theta_{j,k} = 1$, the BSs that offer more resources than the serving BS of user k are identified in the matrix $\Lambda \in \mathbb{R}^{B\times K}$ as follows

$$\Lambda_{j,k} = \begin{cases} 1 & \Omega_j > \Omega_i \\ 0 & \text{otherwise} \end{cases}, \tag{9}$$

The achieved capacity for each candidate pair identified in Λ is then measured

$$\mathbb{C}_{j,k} = \Omega_j.W.\log_2(1 + \Upsilon_{j,k,n}), \tag{10}$$

The set of association pairs that achieve higher capacity than the initial association pair are determined in the matrix $\varpi_{j,k} \in \mathbb{R}^{B\times K}$, where $\varpi_{j,k}$ is set to 1 when the achievable UL capacity at cell j $\mathbb{C}_{j,k}$ is higher than the capacity achieved from the initial association pair and is set to 0 otherwise. The sum throughput is then measured to prioritize the association pairs that maximize the overall network capacity

$$\mathbb{C}_{tot} = \sum_{i=1}^{B}\sum_{k=1}^{K_i}\left\{\Psi_k.W.\log_2(1 + \Upsilon_{i,k,n})\right\}. \tag{11}$$

The process repeats until no further improvement in the network capacity is achieved as shown in Algorithm 1.

B. SINGLE/MULTI-BS ASSOCIATION (SMBA)

The Single/Multi- BS Association (SMBA) scheme determines whether users can connect to multiple BSs or remain connected to only one BS in the UL and DL. Users that are connected to more than one BS can transmit/receive to/from these BSs on different frequency resources simultaneously. Fig. 1 shows a simplified model to illustrate the concept of SMBA, since user u is located in the overlapped area between BSs i and f, user u can be associated with f (in addition to i) if the additional resources occupied by u offered from f do not overlap with other users that might be affected by the interference. To ensure this, the list of users detected in the coverage area of the BSs are determined in both the DL and UL based on equations (4)and (8), respectively. In the DL session, the amount of resources offered from each BS to the users falling within their coverage range is determined in the matrix $\delta \in \mathbb{R}^{B\times K}$

$$\delta_{j,k} = \begin{cases} \Omega_j & \text{if } \Phi_{j,k} = 1 \\ 0 & \text{otherwise} \end{cases}, \forall i, j \in \mathcal{B} \wedge k \in \mathcal{K} \tag{12}$$

Algorithm 1 Coupling/Decoupling Association (CDA)

1: // Candidate association pairs identification
2: $\alpha_{j,k} = \arg\max\left(\Gamma_{k,j}\right)$
3: Calculate Ω_i and Ω_k, Θ and Λ
4: **for** k=1 **until** length(Λ) **do**
5: $\mathbb{C}_{j,k} = \Omega_j.W.\log_2(1 + \Upsilon_{j,k,n})$
6: **if** $\mathbb{C}_{j,k} > \mathbb{C}_{i,k}$ **then**
7: $\varpi_{j,k} = 1$
8: **else**
9: $\varpi_{j,k} = 0$
10: **end if**
11: **end for**
12: // Select among candidate pairs
13: **while** $\mathbb{C}_{tot} > \mathbb{C}_{initial}$
14: **for** t=1 **until** length(ϖ) **do**
15: update association $\alpha_{j,k}$
16: Recalculate Ω_i and Ω_k
17: **if** $\Omega_i + \Omega_j.K_j \leq N$ **then**
18: $\mathbb{C}_{tot} = \sum_{i=1}^{B}\sum_{k=1}^{K_i}\Omega_i.\log_2(1 + \Upsilon_{i,k,n})$
19: **else**
20: Reject association between k and j
21: **end if**
22: **end for**
23: **if** max($\mathbb{C}_{tot}$) > $\mathbb{C}_{initial}$ **then**
24: Final α update
25: **end while**

Similarly, the UL $\delta_{j,k}$ is determined based on Θ. The association mode of a particular user k is determined by checking three conditions where k is allowed to be associated with multiple BSs in the case when none of these conditions are violated. The main target is to ensure that the additional occupied resources by the new association pairs do not cause interference to the surrounding neighbors by orthogonalizing the resources between the interfering BSs/UEs. To demonstrate this, let f and u be a candidate association pair from Φ, the association between f and u can be granted when the three overlap checking conditions are satisfied

$$\psi_{f,u} = \begin{cases} 1, & \text{if C1} \cap \text{C2} \cap \text{C3} \Leftrightarrow 1 \\ 0, & \text{otherwise} \end{cases}, \tag{13}$$

where C1, C2 and C3 represent the conditions to check the orthogonality of resources which are listed as follows

C1: The first condition checks that the additional resources offered from BS f to user u, $\delta_{f,u}$ do not overlap with the resources already allocated to user u denoted by λ_u, from its serving BS i. The orthogonality is maintained by checking that the sum of $\delta_{f,u}$ and λ_u do not exceed the total available resources N as follows

$$\left[\delta_{f,u} + \lambda_u\right] < N, \qquad \begin{matrix} \forall f = 1, \quad \ldots, B, \ldots \\ u = 1, \ldots, K \end{matrix}, \tag{14}$$

C2: The second condition checks the B-dimension in Φ to check that the users connected to the BSs that cover u within

their area are not affected by the new association between BS f and user u.

$$\left[\phi_j + \delta_{f,u} + \lambda_u\right] < N, \qquad \begin{matrix} \forall j, f = 1, \ldots, B, \ldots \\ u = 1, \ldots, K \end{matrix}, \quad (15)$$

where ϕ_j represents the amount of resources occupied by BS j UEs in which j is any BS (except of BS f) that has user u within its coverage range (e.g., BS j from fig. 1).

C3: checks the K-dimension in Φ to make sure that other UEs interfered by BS f (e.g., user k from fig. 1) are not affected by the new association as follows

$$\left[\phi_f + \delta_{f,u} + \lambda_k\right] < N, \qquad \begin{matrix} \forall f = 1, \ldots, B, \ldots \\ u, k = 1, \ldots, K \end{matrix}, \quad (16)$$

where ϕ_f denotes the total occupied resources by BSs f UEs and λ_k denotes the number of resources allocated to user k, in which k is a user interfered by BS f as indicated in Φ.

The impact of associating the pairs that satisfy the conditions in (13) on the network capacity, $\mathbb{C} \in \mathbb{R}^{B \times K}$ is determined for each $\psi_{f,u} = 1$ as follows

$$\mathbb{C}_{f,u} = \sum_{f=1}^{B} \sum_{u=1}^{K_i} \left[\delta_{f,u}.W.\log\left(1 + \Upsilon_{f,u,n}\right)\right]. \quad (17)$$

The priority of selection is then given to the pair that maximizes $\mathbb{C}$ and the process repeats again to search for other association pairs until the capacity can not be maximized further. The association conditions are applied for the UL and DL except for a slight modification in condition 3 in eq. (16) in the UL session, where it is not required to sum λ_k with ϕ_f and $\delta_{f,u}$ as users within BS f's coverage are not affected by the UL interference from user u.

V. HANDOVER RATIO ANALYSIS

The coverage range of BSs plays a key role in making the association decision as discussed in the previous section. Furthermore, the number of users within the coverage area of a BS is highly dependent on the SIR threshold β. Therefore, the impact of the SIR threshold on the percentage of users detected within the coverage range of a cell is investigated in this part. For simplicity, a DL model is considered where the received power from BS i to user k is given by $P_t d_{i,k}^{-\varphi}$ and the received interference power from a nearby BS j to user k is $P_t d_{j,k}^{-\varphi}$, P_t denotes the transmission power, $d_{i,k}$ refers to the distance between BS i and user k and φ is the pathloss exponent. Therefore, user k is located within the coverage area of BS j if

$$\mathcal{P}_t d_{j,k}^{-\varphi} < \frac{\mathcal{P}_t d_{i,k}^{-\varphi}}{\beta}, \quad (18)$$

Assuming all BSs transmit at the same power level, the term in (18) is simplified to

$$\frac{d_{i,k}}{d_{j,k}} < \left(\frac{1}{\beta}\right)^{\frac{1}{\varphi}} \quad (19)$$

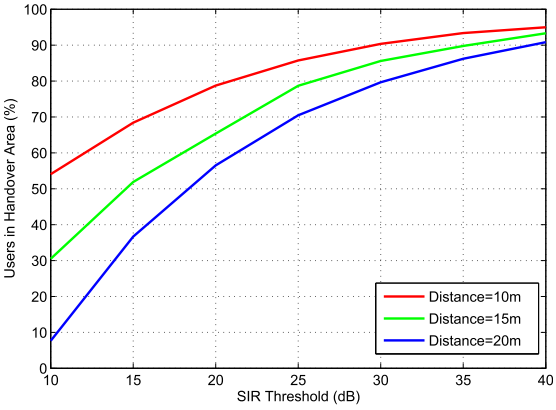

FIGURE 2. Impact of SIR threshold on the percentage of users in the handover area.

where $d_{i,k}/d_{j,k}$ is the distance ratio between BSs i and j and user k which will be referred to as $\mathcal{D}$. The probability density function (PDF) of $\mathcal{D}$ is given by

$$f_{\mathcal{D}}(d) = \begin{cases} f_{\mathcal{D}_1}(d), & \left(\sqrt{2}l_1\right)/\ell < g < \left(\sqrt{l_1^2 + l_2^2}\right)/\ell \\ f_{\mathcal{D}_2}(d), & \left(\sqrt{l_1^2 + l_2^2}\right)/\ell < g < \left(\sqrt{2}l_2\right)/\ell \\ 0, & \text{elsewhere} \end{cases} \quad (20)$$

where $f_{\mathcal{D}_1}(d)$ and $f_{\mathcal{D}_2}(d)$ are shown in (31) and (32).

Please refer to Appendix.

Assume there are f BSs and $\mathcal{S}_f$ users per BS, then the number of users detected in the coverage of BS f can be expressed as

$$\mathcal{U}_f = \mathcal{S}_f + \mathcal{S}_f\,(f-1)\left\{1 - F_{\mathcal{D}_{i,j}}\left(\left(\frac{1}{\beta}\right)^{\frac{1}{\varphi}}\right)\right\} \quad (21)$$

where $F_{\mathcal{D}}\left(d_{i,j}\right)$ represents the cumulative distribution function (CDF) of $f_{\mathcal{D}}\left(d_{i,j}\right)$. Fig. 2 shows that the percentage of users in the handover region can be controlled by varying β. It can be noticed that at higher thresholds, the percentage of users located in the coverage area of the cell is increased as a more users will be detected. The percentage is also seen to increase when the distance is between the cell of interest and the neighboring cells is reduced.

VI. COMPUTATIONAL COMPLEXITY

A. TIME COMPLEXITY

In this section, we measure the complexity of our proposed algorithm in terms of the operations performed, which depends on the number of users deployed in the system. According to Algorithm1, the algorithm starts by computing the capacity for every user in the system based on the number of allocated resources and the SINR. According to [17], the time complexity of Shannon capacity formula is unknown, and therefore we will assume its complexity is given by O(1). Assuming the number of users deployed is given by n, this operation will be executed n times, and therefore the time complexity of the first part of the program

is given by O(1)*n which gives n. As for the second part of the algorithm, for those users achieving more capacity if connected to neighbouring BSs, the overlap condition in line 17 is checked. Since the operation involves a for-loop nested in a while-loop, the computational complexity can be expressed as $n(n+1)$. Therefore, the total time needed can be approximated to $O\left(n^2+2n\right)$. In terms of scale, the number of operations executed depends on the number of deployed users in the network. Therefore, the size of the problem gets larger for larger values of n.

B. SIGNALLING OVERHEAD

The central unit relies heavily on information exchanged with BSs to calculate some parameters needed in our algorithm such as the number of detected users and the allocated resources per user as shown in sec. III. To construct a global view of the network, each BS needs to send its local interference map obtained from (4) to the central unit. The total amount of bits sent from each BS to the central unit, d_i is therefore given by

$$d_i = B.\left(K_i.d_m.J_i\right) \tag{22}$$

where B is the total number of BSs, K_i refers to the number of users served by BS i, d_m denotes the number of bits needed to encode the interference map of BS i and J_i is the number of neighbouring BSs of i. It is worth noting that this sort of arrangement is mostly applicable in interference regions (cell-edge) where the number of cells, and hence users, involved is limited.

VII. RESULTS AND PERFORMANCE ANALYSIS

A. HOMOGENEOUS NETWORK SIMULATION

The performance of the proposed user association scheme is evaluated using a 10 × 10 grid model. Users are randomly and uniformly distributed within the grids with an average of two users per cell. The data rate is evaluated using the adaptive modulation and coding (AMC) technique [18] and the Stanford University Interim (SUI) for Terrain type C is utilized to model the pathloss between BSs and users [19]. The remaining simulation parameters are shown in Table 1.

The NCM user association method is evaluated compared to the standard maximum received signal strength (Max-RSS) association that is implemented with the conventional resource partitioning (CRP) method as well as the IARP approach. In CRP, the allocated resources per BS are measured by dividing the total PRBs by the number of detected users. Furthermore, the reuse-1 system is used as a benchmark for comparison. In reuse-1, each cell utilizes the entire available bandwidth without applying ICIC to manage the inter-cell interference. Fig. 3 shows a throughput CDF where it is shown that the NCM method achieves superior performance compared to the other techniques.

The adaptive decoupling and multi-BS association method is also evaluated in this section. Since the DL rate is not affected by the decoupling, as users in the DL follow the Max-RSS association policy, the impact of CDA method

TABLE 1. Simulation parameters.

Parameter	Value	Parameter	Value
Carrier (f_c)	2.3 GHz	Bandwidth	5/10 MHz
Resource blocks (RB)	25/50	Thermal Noise Density	-174 dBm/Hz
OFDM symbol period	1.43×10^{-4}s	Log normal shadowing	8 dB
Number of Macrocells	1	Number of Picocells	10
Macrocell Tx Power	46 dBm	Picocell Tx Power	30 dBm
Femtocell Tx Power	20 dBm	Macrocell UEs distribution Radius	289 m (Inter-Site distance= 500m)
Picocell UEs distribution Radius	40 m	Femtocell UEs distribution Radius	10 m
Minimum Distance Macro-Pico	75 m	Minimum Distance Pico-Pico	30 m
Minimum Distance Macro-UE	35 m	Minimum Distance Pico-UE	10 m

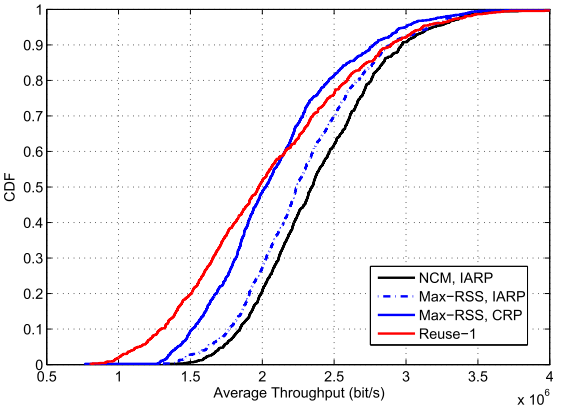

FIGURE 3. DL cumulative distribution function of the average throughput comparison of the NCM association with 2 UEs per femtocell.

is evaluated in the UL only whereas the SMBA method is evaluated in both sessions. The single-BS association (SBA) is used as a benchmark to show the gain achieved by the SMBA method. In SBA, users are allowed to connect to only one BS based on the Max-RSS strategy in the DL and on the CDA method in the UL. The method in [20] is also used as a benchmark for comparison, where users connect to the BS with the minimum pathloss. Fig. 4 shows the UL average rate per user performance comparison at various femtocell densities. To show the gain achieved from decoupling the UL user association from the DL association, the SBA is evaluated with coupled and decoupled associations separately where it is shown that about 12% improvement can be achieved by decoupling the UL association from the DL. The figure also shows that the proposed adaptive CDA and SMBA method provides significant data rate improvement especially at lower densities of femtocells. Fig. 5 illustrates the CDF of the UL user throughput. It can be seen that the user throughput is considerably improved with our proposed method due to the increased resource utilization

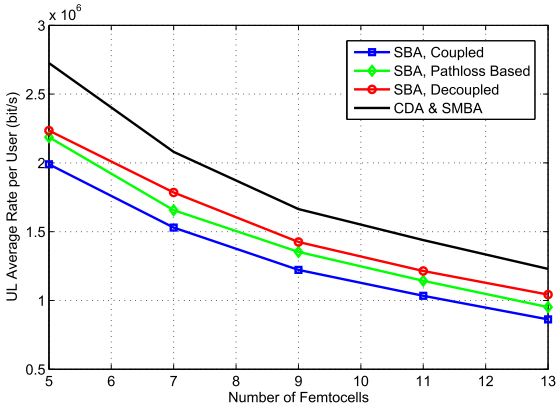

FIGURE 4. UL data rate per user performance of adaptive CDA and SMBA scheme with 2 UEs per femtocell.

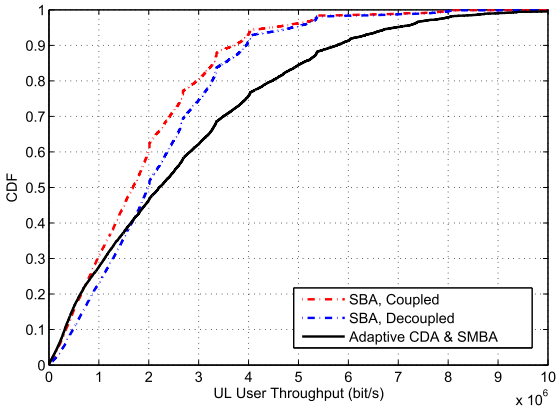

FIGURE 5. Cumulative distribution function of the UL user throughput of the adaptive CDA and SMBA scheme with 2 UEs per femtocell.

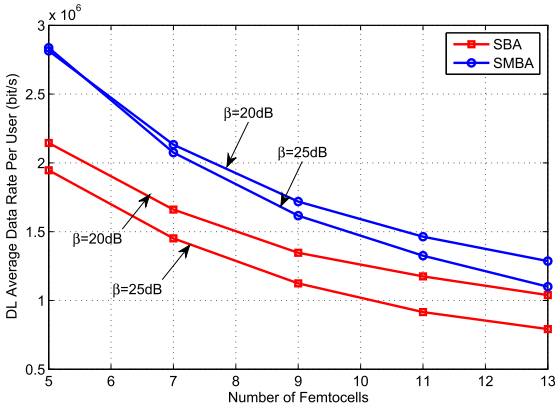

FIGURE 6. DL data rate per user performance comparison between SBA and SMBA schemes with 2 UEs per femtocell.

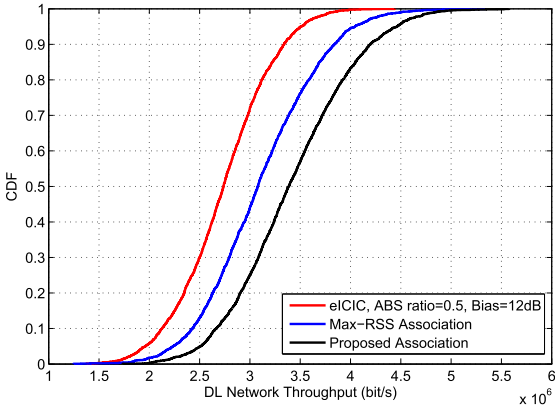

FIGURE 7. Cumulative distribution function of the heterogeneous network DL throughput.

of the network. However, the figure shows slight degradation for a small percentage of cell-edge users due to the increased generated interference resulting from increasing the total frequency reuse. Fig. 6, shows the DL data rate per user performance vs. the total number of deployed femtocells. The figure compares the performance of our proposed SMBA with SBA where it is shown that our proposed method can achieve remarkable improvement compared to SBA due to the increased resource utilization in the system. It can also be noticed that the performance gap between the SMBA method and SBA reduces as the number of BSs increase due to the increased interference which limits the resource utilization. The methods are also evaluated by varying the SIR threshold β. According to the method in [21], higher β cause the data rate to reduce as BSs detect more interfered neighboring users within their coverage which cause BSs to decrease their resource utilization to avoid the interference. Fig. 6 also shows that the performance gap between the two thresholds is wider in SBA than SMBA. This is because SMBA provides better resource utilization especially at low femtocell density, where the interference is lower and the impact of higher β values reduces. However, as the number of cells increase, the interference becomes higher causing the data rate to reduce gradually.

B. HETEROGENEOUS NETWORK SIMULATION

In this part, we consider a macrocell network overlaid with 10 outdoor picocells uniformly distributed in the coverage area of the macrocell. A total of 30 UEs are deployed with 2/3 of the UEs generated in hotspots within a 40 m radius from the picocells and the rest of the users are randomly and uniformly dropped within the macrocell coverage [22]. A 10 MHz bandwidth is utilized n with 50 PRBs dedicated for data transmission. The performance of the proposed method is evaluated in heterogeneous network scenario compared to state-of-art techniques in which all techniques apply small cell biasing to achieve cell range extension. To manage the cross-tier interference, frequency domain eICIC scheme is used where resources are orthogonalized between the two layers in the frequency domain. A joint resource partitioning and offloading scheme is performed where a fraction of resources to be used by the macrocell is determined according to the total offloaded users [23].

Fig. 7 shows the average DL network throughput per user CDF. The NCM association is compared with the standard Max-RSS association in addition to enhanced inter-cell interference coordination (eICIC) scheme that is used as a benchmark with an almost blank subframe (ABS)

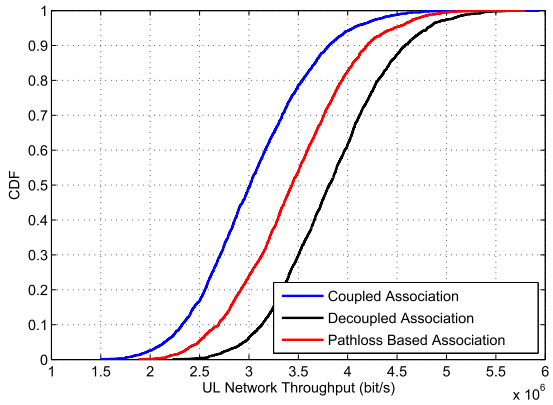

FIGURE 8. Cumulative distribution function of the heterogeneous network UL throughput.

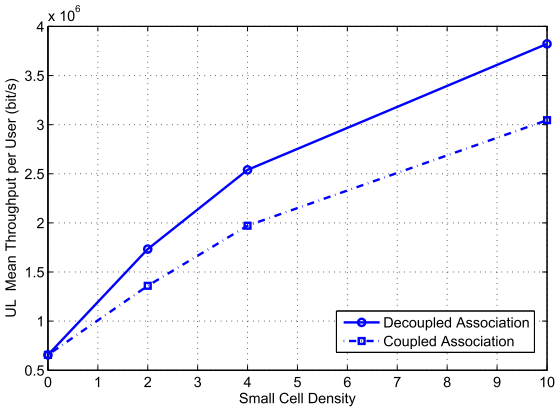

FIGURE 9. Heterogeneous network UL rate vs. the number of deployed small cells.

ratio of 50%. Note that all schemes including the eICIC method apply range extension bias of 12 dB for traffic offloading. The figure shows that the NCM association technique provides better performance in comparison with the other schemes with around 20% improvement when compared with the Max-RSS association. The reason for this improvement is is that the macrocell users associate with the underutilized small cells where they enjoy a wider range of frequency resources compared to the resources offered from the overloaded macrocell. Furthermore, UEs of loaded small cells may associate with less loaded small cells to acquire more resources. Fig. 8 shows the average UL throughput CDF where a comparison is conducted between coupled, decoupled and pathloss based association. In coupled association, users connect with BSs based on the DL Max-RSS association whereas in decoupled association, the UL association is decoupled from the DL association and the association is performed based on the coupling/decoupling association (CDA) method. The minimum pathloss based association in [20] is also used as a benchmark for comparison. It can be seen from the figure that the proposed decoupling approach provide significant improvement compared to the coupled case. Following the DL association in the UL is inefficient, since the majority of users are forced to connect to the macrocell due to the high transmission power which increases the traffic load on the macrocell leaving the small cells underutilized. However, when the proposed decoupling is applied, the traffic is offloaded from the macrocell to the small cells where better resource utilization can be achieved. Furthermore, the proposed decoupling scheme outperforms the pathloss based association approach since with pathloss based association, users associate with the cells with the minimum pathloss without considering other factors such as the cell loads. Fig. 9 shows the impact of varying the small cell density within the macrocell coverage on the UL mean throughput per user. It can be seen that as the number of deployed small cell increases, the average rate increases. This is because, adding more small cells means more users are offloaded from the macrocell to the small cells in which they are granted more resources compared to the resources offered from the congested macrocell. Additionally, from a co-tier perspective, the proposed decoupled association is more effective at higher density of small cells. This is because of the increased overlapped regions at higher densities, which provide more flexibility for users to be handed-off to less loaded cells.

VIII. CONCLUSION

This paper introduced a novel adaptive decoupling and Multi-BS association framework for enhancing capacity in cellular communication systems. The proposed algorithms were shown to significantly increase the system's frequency reuse by carefully exploiting a wider range of options for associating users and base-stations to be able to glean further improvements from underutilized resources in the network. To ensure that no associations result in increasing interference, an overlap checking scheme is proposed to enforce a set of conditions before deciding whether to grant or deny certain associations. The results demonstrate that the decoupling performance is very sensitive to the deployment scenarios, especially in heterogeneous networks, due to reasons such as transmission power differences and the number of deployed small cells amongst other, which makes it essential to adapt to such diversities. The results also show that our proposed method improves the overall throughput by almost 15% compared to the benchmark techniques, without compromising QoS.

APPENDIX

The downlink SIR probability density function (PDF) is conditionally derived based on the location of the user to provide an accurate modelling of the received interference [24]. Assume a grid model is used in which two BSs referred to as P_1 and P_2 are placed in the centre of each grid. P_1 and P_2 are considered to be located on the x,y-place where P_1 is positioned at the origin, and P_2 is placed at a fixed distance relative to P_1 which is denoted by ℓ at position (x_{p_2}, y_{p_2}). Consider a user m, which is presumed to be distributed in a uniform and random manner and given by the location (r, θ), where $0 < r \leq R$ and $0 \leq \theta \leq 2\pi$. If we assume that r and θ

$$f_{D_1}(d) = \frac{d\ell p_1^2}{8}[2l_1\sqrt{(d\ell)^2 - l_1^2}\left((d\ell)^2 - 2l_1^2\right) + (d\ell)^4 \arctan\left(\frac{\sqrt{(d\ell)^2 - l_1^2}}{(d\ell)}\right) - (d\ell)^4 \arctan\left(\frac{l_1}{\sqrt{(d\ell)^2 - l_1^2}}\right)] + \frac{d\ell p_2^2}{2}\left[(d\ell)^2 - 2l_1^2\right]$$
$$\times d\ell p_1 p_3\left[(d\ell)^2 \arctan\left(\frac{\sqrt{(d\ell)^2 - l_1^2}}{l_1}\right) - (d\ell)^2 \arctan\left(\frac{l_1}{\sqrt{(d\ell)^2 - l_1^2}}\right)\right] + 2d\ell p_2 p_3\left[\sqrt{(d\ell)^2 - l_1^2} - l_1\right] \quad (31)$$

$$f_{D_2}(d) = \frac{d\ell p_1^2}{8}[2l_2\sqrt{(d\ell)^2 - l_2^2}\left(l_2^2 - (d\ell)^2\right) + (d\ell)^4 \arctan\left(\frac{l_2}{\sqrt{(d\ell)^2 - l_2^2}}\right) - (d\ell)^4 \arctan\left(\frac{\sqrt{(d\ell)^2 - l_2^2}}{l_2}\right)] + \frac{d\ell p_2^2}{2}\left[2l_2^2 - (d\ell)^2\right]$$
$$+ d\ell p_1 p_3\left[(d\ell)^2 \arctan\left(\frac{l_2}{\sqrt{(d\ell)^2 - l_2^2}}\right) - (d\ell)^2 \arctan\left(\frac{\sqrt{(d\ell)^2 - l_2^2}}{l_2}\right)\right] + 2d\ell p_2 p_3\left[l_2 - \sqrt{(d\ell)^2 - l_2^2}\right] \quad (32)$$

are uniformly distributed random variables, the PDF of r, $f_R(r)$, is given by

$$f_R(r) = \begin{cases} \frac{1}{R}, & 0 < r \leq R \\ 0, & \text{elsewhere} \end{cases} \quad (23)$$

And the PDF of θ, $f_\phi(\theta)$ is expressed as

$$f_\phi(\theta) = \begin{cases} \frac{1}{2\pi}, & 0 \leq \theta \leq 2\pi \\ 0, & \text{elsewhere} \end{cases} \quad (24)$$

The polar coordinates r and θ can be transformed to Cartesian coordinates x and y using trigonometric functions

$$x = r.cos(\theta) \quad (25)$$
$$y = r.sin(\theta) \quad (26)$$

Using change-of-variable method, the random variable θ is transformed into the form $cos(\theta)$ as follows

$$f_Z(z) = \begin{cases} \frac{1}{\pi\sqrt{1-z^2}}, & -1 < z < 1 \\ 0, & elsewhere \end{cases} \quad (27)$$

In a similar fashion, the pdf of the transformation of $sin(\theta)$ can be expressed as

$$f_V(v) = \begin{cases} \frac{1}{\pi\sqrt{1-v^2}}, & -1 < v < 1 \\ 0, & \text{elsewhere} \end{cases} \quad (28)$$

The pdf, $f_X(x)$ as described in (25) is given by

$$f_X(x) = \int_{-\infty}^{+\infty} f_{Z/X}\left(\frac{z}{x}\right).f_Z(x).\frac{1}{x}dx \quad (29)$$

where $X = Z$ and $\frac{Z}{X} = R$ and the PDF of x is given by

$$f_X(x) = \begin{cases} \frac{1}{\pi R}.\{\log(R) - \log(x) + \\ \quad \log\left(1 + \sqrt{1 - \frac{x^2}{R^2}}\right)\} & -R \leq x \leq R/\{0\} \\ 0, & \text{elsewhere} \end{cases} \quad (30)$$

The euclidean distance between the BS P_2 and the user m is stated as

$$G = \sqrt{\Delta x^2 + \Delta y^2} \quad (33)$$

In which $\Delta x = x - x_{p_2}$ and $\Delta y = y - y_{p_2}$

Using change-of-variable, the pdf of Δx, $f_{\Delta x}(x)$ can be expressed as

$$f_{\Delta X}(x) = \begin{cases} \frac{1}{\pi R}.\{\log(R) - \log(x - a) & a-R \leq x \leq a+R/\{a\} \\ + \log\left(1 + \sqrt{1 - \frac{(x-a)^2}{R^2}}\right)\} & \\ 0 & \text{elsewhere} \end{cases} \quad (34)$$

Similarly, the pdf of Δy, $f_{\Delta y}(y)$ is given by

$$f_{\Delta Y}(y) = \begin{cases} \frac{1}{\pi R}.\{\log(R) - \log(y - a) & a-R \leq y \leq a+R/\{a\} \\ + \log\left(1 + \sqrt{1 - \frac{(y-a)^2}{R^2}}\right)\} & \\ 0 & \text{elsewhere} \end{cases} \quad (35)$$

The joint probability density of Δx and Δy is given by

$$f_{\Delta X,\Delta Y}(x, y) = f_{\Delta X}(x).f_{\Delta Y}(y) \quad (36)$$

The probability density function of G, $f_G(g)$ as defined in (33) is given by

$$f_G(g) = \int_{-\infty}^{+\infty} |\frac{g}{\sqrt{g^2 - x^2}}|.f_{\Delta X,\Delta Y}\left(x, \sqrt{g^2 - x^2}\right) \quad (37)$$

To simplify the analysis, the expressions in (34) and (35) are transformed into quadratic form

$$f_{\Delta X}(x) = p_1 x^2 + p_2 x + p_3 \quad (38)$$
$$f_{\Delta Y}(y) = p_1\left(g^2 - x^2\right) + p_2\sqrt{g^2 - x^2} + p_3 \quad (39)$$

Therefore, the probability density function of G, $f_G(g)$ can be expressed as

$$f_G(g) = \begin{cases} f_{G_1}(g), & \sqrt{2}l_1 < g < \sqrt{l_1^2 + l_2^2} \\ f_{G2}(g), & \sqrt{l_1^2 + l_2^2} < g < \sqrt{2}l_2 \\ 0, & elsewhere \end{cases} \quad (40)$$

where $l_1 = a - R$, $l_2 = a + R$ and $f_{G_1}(g), f_{G_2}(g)$ are given by (41) and (42)

$$\begin{aligned} & f_{G_1}(g) \\ & = 2gp_2p_3\left[\sqrt{g^2-l_1^2}-l_1\right]+\frac{gp_2^2}{2}\left[g^2-2l_1^2\right] \\ & \quad + gp_1p_3\left[g^2\arctan\left(\frac{\sqrt{g^2-l_1^2}}{l_1}\right)\right. \\ & \quad \left. -g^2\arctan\left(\frac{l_1}{\sqrt{g^2-l_1^2}}\right)\right] \\ & \quad + \tfrac{gp_1^2}{8}[2l_1\sqrt{g^2-l_1^2}\left(g^2-2l_1^2\right)+g^4\arctan\left(\frac{\sqrt{g^2-l_1^2}}{g}\right) \\ & \quad - g^4\arctan\left(\frac{l_1}{\sqrt{g^2-l_1^2}}\right)] \end{aligned} \tag{41}$$

$$\begin{aligned} & f_{G_2}(g) \\ & = 2gp_2p_3\left[l_2-\sqrt{g^2-l_2^2}\right]+\tfrac{gp_2^2}{2}\left[2l_2^2-g^2\right] \\ & \quad + gp_1p_3\left[g^2\arctan\left(\frac{l_2}{\sqrt{g^2-l_2^2}}\right)\right. \\ & \quad \left. -g^2\arctan\left(\frac{\sqrt{g^2-l_2^2}}{l_2}\right)\right] \\ & \quad + \tfrac{gp_1^2}{8}[2l_2\sqrt{g^2-l_2^2}\left(l_2^2-g^2\right)+g^4\arctan\left(\frac{l_2}{\sqrt{g^2-l_2^2}}\right) \\ & \quad - g^4\arctan\left(\tfrac{l_1}{\sqrt{g^2-l_1^2}}\right)] \end{aligned} \tag{42}$$

The distance ratio between P_1, P_2 and m is defined as $\mathcal{D} = G/\ell$. Therefore, the pdf of $f_D(d)$ can be expressed as

$$f_D(d) = \begin{cases} f_{D_1}(d), & \left(\sqrt{2}l_1\right)/\ell < g < \left(\sqrt{l_1^2+l_2^2}\right)/\ell \\ f_{D_2}(d), & \left(\sqrt{l_1^2+l_2^2}\right)/\ell < g < \left(\sqrt{2}l_2\right)/\ell \\ 0, & \textit{elsewhere} \end{cases} \tag{43}$$

where $f_{D_1}(d)$ and $f_{D_2}(d)$ are given by (31) and (32), as shown at the top of the previous page.

REFERENCES

[1] X. Chu, D. Lopez-Perez, Y. Yang, and F. Gunnarsson, *Heterogeneous Cellular Networks: Theory, Simulation and Deployment*, 2nd ed. Cambridge, MA, USA: Cambridge Univ. Press, 2008.

[2] D. Lopez-Perez, A. Valcarce, G. de la Roche, and J. Zhang, "OFDMA femtocells: A roadmap on interference avoidance," *IEEE Commun. Mag.*, vol. 47, no. 9, pp. 41–48, Sep. 2009.

[3] D. Prajapati and V. Richhariya, "A survey on cell selection schemes for femtocell networks," in *Proc. IEEE Pers. Indoor Mobile Radio Commun. (PIMRC)*, Jul. 2014, pp. 465–468.

[4] M. Wang, X. Zhu, Z. Zeng, S. Wan, and W. Li, "System performance analysis of OFDMA-based femtocell networks," in *Proc. IET Int. Conf. Commun. Technol. Appl. (ICCTA)*, Oct. 2011, pp. 405–410.

[5] H. Zhou, D. Hu, S. Mao, P. Agrawal, and S. A. Reddy, "Cell association and handover management in femtocell networks," *CoRR*, Oct. 2012.

[6] A. Ebrahim and E. Alsusa, "Interference minimization through sleep mode based resource allocation for future femtocell networks," in *Proc. IEEE Int. Conf. Commun. (ICC)*, Jun. 2015, pp. 1679–1684.

[7] R. Madan, J. Borran, A. Sampath, N. Bhushan, A. Khandekar, and T. Ji, "Cell association and interference coordination in heterogeneous LTE-A cellular networks," *IEEE J. Sel. Areas Commun.*, vol. 28, no. 9, pp. 1479–1489, Dec. 2010.

[8] J. Sangiamwong, Y. Saito, N. Miki, T. Abe, S. Nagata, and Y. Okumura, "Investigation on cell selection methods associated with inter-cell interference coordination in heterogeneous networks for LTE-advanced downlink," in *Proc. 11th Eur. Wireless Conf. Sustain. Wireless Technol. (Eur. Wireless)*, Apr. 2011, pp. 1–6.

[9] F. Boccardi *et al.*, "Why to decouple the uplink and downlink in cellular networks and how to do it," *CoRR*, Mar. 2015.

[10] H. Elshaer, F. Boccardi, M. Dohler, and R. Irmer, "Load & backhaul aware decoupled downlink/uplink access in 5G systems," in *Proc. IEEE Int. Conf. Commun.*, Jun. 2015, pp. 5380–5385.

[11] W. Saad, Z. Han, R. Zheng, M. Debbah, and H. V. Poor, "A college admissions game for uplink user association in wireless small cell networks," in *Proc. IEEE INFOCOM*, Apr. 2014, pp. 1096–1104.

[12] S. Singh, X. Zhang, and J. G. Andrews, "Joint rate and SINR coverage analysis for decoupled uplink-downlink biased cell associations in HetNets," *IEEE Trans. Wireless Commun.*, vol. 14, no. 10, pp. 5360–5373, Oct. 2015.

[13] T. F. Rahman, C. Sacchi, and C. Schlegel, "Link performance analysis of cooperative transmission techniques for LTE-A uplink," in *Proc. IEEE Aerosp. Conf.*, Mar. 2015, pp. 1–8.

[14] G. Nauryzbayev and E. Alsusa, "Interference alignment cancellation in compounded MIMO broadcast channels with general message sets," *IEEE Trans. Commun.*, vol. 63, no. 10, pp. 3702–3712, Oct. 2015.

[15] A. Ebrahim and E. Alsusa, "Joint interference aware resource partitioning and cellular association for femtocell networks," in *Proc. IEEE Globecom*, Dec. 2015, pp. 1679–1684.

[16] Y. Zhou, F. Meshkati, V. Makh, Y. Tokgoz, and M. Yavuz, "Uplink interference management techniques for 3G femtocells," in *Proc. IEEE 22nd Int. Symp. Pers. Indoor Mobile Radio Commun. (PIMRC)*, Sep. 2011, pp. 16–20.

[17] M. Fallgren, "On the complexity of maximizing the minimum shannon capacity in wireless networks by joint channel assignment and power allocation," in *Proc. IEEE 18th Int. Workshop Quality Service (IWQoS)*, Jun. 2010, pp. 1–7.

[18] *Technical Specification Group Radio Access Network; Physical Layer Aspects of UTRA High Speed Downlink Packet Access*, document TR 25.848, 3GPP, 3rd Generation Partnership Project (3GPP), Mar. 2001.

[19] S. S. Jeng, J. M. Chen, C. W. Tsung, and Y. F. Lu, "Coverage probability analysis of IEEE 802.16 system with smart antenna system over Stanford University interim fading channels," *IET Commun.*, vol. 4, no. 1, pp. 91–101, Jan. 2010.

[20] H. Elshaer, F. Boccardi, M. Dohler, and R. Irmer, "Downlink and uplink decoupling: A disruptive architectural design for 5G networks," in *Proc. IEEE Global Commun. Conf. (GLOBECOM)*, Dec. 2014, pp. 1798–1803.

[21] W. Pramudito and E. Alsusa, "A hybrid resource management technique for energy and QoS optimization in fractional frequency reuse based cellular networks," *IEEE Trans. Commun.*, vol. 61, no. 12, pp. 4948–4960, Dec. 2013.

[22] *Evolved Universal Terrestrial Radio Access (E-UTRA); Further Advancements for E-UTRA Physical Layer Aspects*, document TS 36.814, 3GPP, 3rd Generation Partnership Project (3GPP), Mar. 2010.

[23] S. Singh and J. G. Andrews, "Joint resource partitioning and offloading in heterogeneous cellular networks," *IEEE Trans. Wireless Commun.*, vol. 13, no. 2, pp. 888–901, Feb. 2014.

[24] A. Ebrahim and E. Alsusa, "Interference and resource management through sleep mode selection in heterogeneous networks," *IEEE Trans. Commun.*, vol. 65, no. 1, pp. 257–269, Jan. 2017.

AYSHA EBRAHIM received the B.Sc. degree in computer engineering from University of Bahrain in 2009, the M.Sc. degree in electronic engineering from University of York in 2011, and the Ph.D. degree in electrical and electronic engineering from The University of Manchester in 2016. She is currently with the Department of Computer Engineering, University of Bahrain, as an Assistant Professor. Her research focuses on radio resource management techniques for heterogeneous wireless networks.

EMAD ALSUSA (SM'07) received the Ph.D. degree in telecommunications from the University of Bath in 2000. In 2000, he became a Post-Doctoral Research Associate with Edinburgh University. He joined Manchester University in 2003, as a Full Faculty Member. His research interest lies in the area of signal processing and communication theory with a focus on the physical and MAC layers of wireless communication networks for which he designs advanced algorithms for energy and spectrum optimization in the presence of interference and various channel nonlinearities. His research work has so far resulted in well over a 150 journal and refereed conference publications mainly in the top IEEE venues. He is a fellow of the U.K. Higher Academy of Education. He was a co-recipient of the best paper award in the International Symposium on Power Line Communications, in 2014. He has volunteered for various IEEE activities, including the VTC TPC Co-Chair of the Greencom Track in VTC 2016 and the General Co-Chair of the Online Green Com Conference in 2016.